m*l*) of the whole-cell antigens (optical density of 0.8 at 450 nm) and serum, which had been serially diluted 2-fold with PBS were incubated at 50°C for 24 hr. Agglutination titers were determined from the final dilution of serum showing 50% agglutination. Samples showing a titer higher than 160 were considered to be positive [3].

Canine sera: Serum samples (n=318) were randomly selected from dogs consecutively admitted to animal hospitals in central Japan by hospital staff in 2006. *B. canis* infected sera were collected from PCR positive dogs, and *B. canis* free sera were collected from SPF dogs.

SDS-PAGE and Western blotting: The antigen solution was separated using 10% SDS-PAGE and then transferred to Immobilon-P membranes (Millipore). The efficiency of transfer was determined using Coomassie brilliant blue R-250 and then the membranes were tested for reactivity with antibodies in *B. canis* infected sera that were collected from PCR positive dogs. Protein bands were cut out from the membranes and the N-terminal amino acid sequences were analyzed at TAKARA Biotechnology Co.

PCR: Blood samples were collected from tube agglutination test positive dogs, and then DNA specimens prepared using a QIAamp DNA Blood Kit (QIAGEN) for the PCR amplification assay to detect *B. canis*. Specific primer sequences were designed to detect the *virB2* gene for *Brucella* spp. [6, 13].

RESULTS

Latex bead agglutination test: We coated latex beads with antigens from a hot saline extract of *B. canis* with the aim of achieving a serodiagnosis method that is faster and easier to perform. *B. canis* infected serum from dogs, in which infection had been confirmed by the tube agglutination test and PCR, was mixed with the antigen coated latex beads and this mixture incubated at room temperature for 15 min. Agglutination was clearly observed (Fig. 1). On the other hand, *B. canis* free dog serum showed no agglutination (Fig. 1). When the latex bead agglutination test was conducted for twelve different *B. canis* infected or non-infected dog sera, we obtained the same results.

Analysis of hot saline extracted antigens: The antigens extracted with hot saline were analyzed by Western blotting with dog serum infected with *B. canis*. In the separation of proteins by SDS-PAGE, four protein bands reacted with the serum (Fig. 2). Antigen 3 (Ag 3 in Fig. 2) showed high immuno-reactivity and another three antigens showed similar reactivity. Although a further protein band at around 10 kDa reacted with the serum, this band was not separated completely judging by Coomassie blue staining. To identify the genes encoding the antigens, their N-terminal amino acid sequences were analyzed and the homologous proteins searched on a database. The results are shown in Table 1. Three proteins could be analyzed and corresponded with GenBank's *Brucella* genome database, but one of the proteins (antigen 2) could not be analyzed.

Comparison of latex bead and tube agglutination tests: A serological survey of canine sera collected in Japan was conducted by both the latex bead and tube agglutination tests in order to compare them. Antibodies to *Brucella* were detected by the tube agglutination test in 41 of 318 serum samples and by the latex bead agglutination test in 12 of 318 serum samples that tested positive (Table 2). No sample determined to be negative by the tube agglutination test showed positive by the latex bead agglutination test. Genetic diagnosis of dog sera shown to be positive or negative by the latex bead agglutination test by PCR showed that 5 of the 12 samples (47.1%) or 0 of the 29 samples (0%) were positive (Table 2).

DISCUSSION

The tube agglutination test with whole *B. canis* antigens has been used to diagnose brucellosis in dogs in Japan [11]. However, nonspecific reactions occur in the tube agglutination test using whole bacterial cell antigens as well as in the

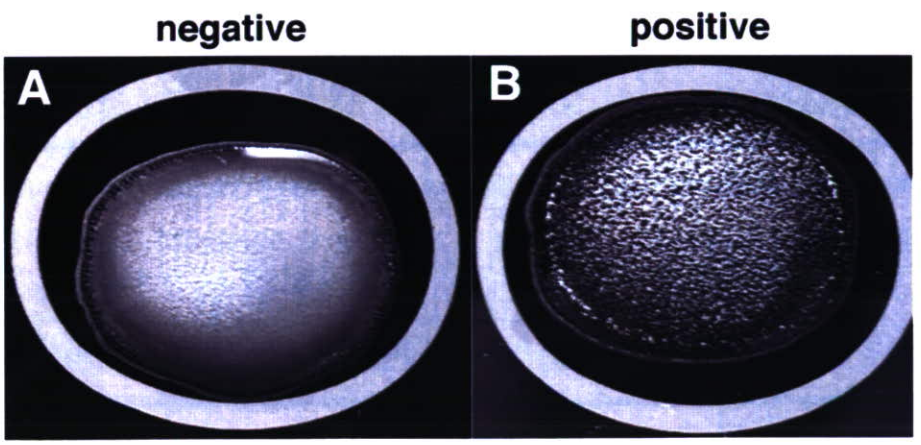

Fig. 1. Latex bead agglutination test. *B. canis* free (A) and infected (B) sera were mixed with beads coated with antigen from a crude hot saline extract. Agglutination is clearly observed in panel B.

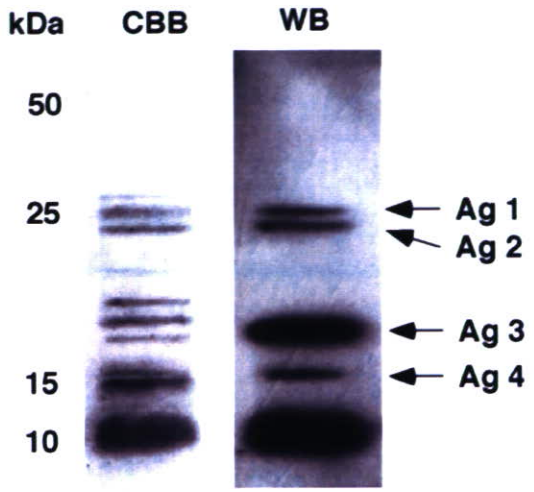

Fig. 2. Western blot analysis of crude hot saline extracts. Antigens were separated by SDS-PAGE and then transferred to the nylon membranes. The membranes were stained with Coomassie brilliant blue (CBB) and used for analysis of *B. canis* infected serum (WB). Four antigens were detected (Ag 1–4).

Table 1. Antigens contained in hot saline extract

Antigens	Gene products (putative function)	GenBank accession No.
Ag 1	Ribose ABC transporter	AAN34031.1
Ag 2	Unanalyzable	
Ag 3	Superoxide dusmutase Cu-Zn	AAN33888.1
Ag 4	Hypothetical protein	AAX74222.1

Table 2. Serological analysis of canine sera

	TAT[a] +		TAT −	
	LB[b]+	LB−	LB+	LB−
Sera (n=318)	12 (3.8%)	29 (9.1%)	0 (0%)	277 (87.1)
PCR+ in TAT+	5 (41.7%)	0 (0%)	−	−

a) Tube agglutination test.
b) Latex bead agglutination test.

rapid slide agglutination test [2]. With the aim of developing a serological diagnosis method that is easier to perform, latex beads were coated with antigens extracted by hot saline for use in an agglutination test. Though crude hot saline antigen extracts had been used previously for a gel immunodiffusion test [12], the antigens contained in the extracts had not been clearly identified. In the present study, we were able to detect four antigens and three could be identified. Since Copper-zinc superoxide dismutase (Cu-Zn SOD) is a known antigenic protein of *Brucella abortus* and there is also Cu-Zn SOD in *B. canis* [1], its potential value as a vaccine for brucellosis prevention and diagnostic reagent for the disease has been investigated [9, 10]. This suggests that purified Cu-Zn SOD could be a useful antigen for the specific serological diagnosis of canine brucellosis. The other antigens, ribose ABC transporter (antigen 1) and hypothetical protein (antigen 4), have not previously been reported to be *B. canis* antigens. Since these proteins show lower reactivity than Cu-Zn SOD against *B. canis* infected dog serum, it is unclear whether, as purified single proteins, they would be suitable for the serological diagnosis of brucellosis or not. Thus the antigenic properties of these newly identified antigens need to be properly characterized. Since the N-terminal of antigen 2 was blocked, its amino acid sequence could not be determined by our method.

The cross-reactivity between *B. canis* and other pathogens in serological tests is still not fully understood [2]. To investigate the specificity of crude hot saline antigen extracts in this respect, an enzyme-linked immunosorbent assay (ELISA) was performed with the above antigens. Unexpectedly, the ELISA reactions with the crude hot saline antigen extracts for both *B. canis* infected and non-infected dog sera were similar (data not shown). This suggests that the crude hot saline extracts were not specific antigens and therefore not useful with a highly sensitive serodiagnosis method such as ELISA. Since the latex bead agglutination test is a less sensitive method than ELISA, we consider that the results obtained with the latex bead agglutination test clearly show the difference between positive and negative.

In surveys of canine brucellosis performed in the same area as that investigated in this study in 1977 and 1989, 2.5 and 1.5% of the dogs were positive, respectively [11, 12]. Since our results show an increase in the percentage of positive dogs for brucellosis as compared to the previous surveys, we should continue to investigate the seroprevalence of *B. canis* in dogs in order to monitor for epidemics of canine brucellosis in Japan.

Our latex bead agglutination test is user-friendly, needs no special equipment and requires little or no technical skill. The result is obtained within 15 min and the test can be performed under field conditions. Although our results show that the latex bead agglutination test is useful in the serological diagnosis of canine brucellosis, more studies are required in order for it to be approved as a diagnostic tool for canine brucellosis. This will involve testing a large number of serum samples from areas where there are brucellosis epidemics and those that are brucellosis free, as well the large-scale testing of samples from bacteriologically positive dogs.

ACKNOWLEDGEMENTS. We thank Dr. Alexander Cox for his critical reading of the manuscript. This work was supported by grants from the Special Coordination Funds for Promoting Science and Technology, Ministry of Education, Culture, Sports, Science and Technology.

REFERENCES

1. Bricker, B. J., Tabatabai, L. B., Judge, B. A., Deyoe, B. L. and Mayfield, J. E. 1990. Cloning, expression, and occurrence of the *Brucella* Cu-Zn superoxide dismutase. *Infect. Immun.* **58**: 2935–2939.

2. Corbel, M. J. 1985. Recent advances of *Brucella* antigens and their serological cross-reactions. *Vet. Bull.* **55**: 927–942.
3. Erdenebaatar, J., Bayarsaikhan, B., Watarai, M., Makino, S. and Shirahata, T. 2003. Enzyme-linked immunosorbent assay to differentiate the antibody responses of animals infected with *Brucella* species from those of animals infected with *Yersinia enterocolitica* O9. *Cln. Diag. Lab. Immnol.* **10**: 710–714.
4. Flores-Castro, R. and Carmichael, L. E. 1978. VI. Canine brucellosis. Current status of methods for diagnosis. *Cornell Vet.* **68**: 76–88.
5. George, L. W. and Carmichael, L. E. 1974. A plate agglutination test for the rapid diagnosis of canine brucellosis. *Am. J. Vet. Res.* **35**: 905–909.
6. Kim, S., Lee, D. S., Suzuki, H. and Watarai, M. 2006. Detection of *Brucella canis* and Leptospira interrogans in canine semen by multiplex nested PCR. *J. Vet. Med. Sci.* **68**: 615–618.
7. Myers, D. M., Varela-Diaz, V. M. and Coltorti, E. A. 1974. Comparative sensitivity of gel-diffusion and tube agglutination tests for the detection of *Brucella canis* antibodies in experimentally infected dogs. *Appl. Microbiol.* **23**: 894–902.
8. Nielsen, K. H. and Duncan, J. R. 1990. Animal Brucellosis. CRC Press, Boca Raton.
9. Onate, A. A., Vemulapalli, R., Andrews, E., Schurig, G. G., Boyle, S. and Folch, H. 1999. Vaccination with live *Escherichia coli* expressing *Brucella abortus* Cu/Zn superoxide dismutase protects mice against virulent *B. abortus*. *Infect. Immun.* **67**: 986–988.
10. Onate, A. A., Cespedes, S., Cabrera, A., Rivers, R., Gonzalez, A., Munoz, C., Folch, H. and Andrews, E. 2003. A DNA vaccine encoding Cu,Zn superoxide dismutase of *Brucella abortus* induces protective immunity in BALB/c mice. *Infect. Immun.* **71**: 4857–4861.
11. Serikawa, T., Muragichi, T. and Nakano, N. 1977. A survey of dogs from Gifu and Shiga areas for *Brucella canis*. *Jpn. J. Vet. Sci.* **39**: 635–642.
12. Serikawa, T., Iwaki, S., Mori, M., Muraguchi, T. and Yamada, J. 1989. Purification of a *Brucella canis* cell wall antigen by using immunosorbent columns use of the antigen in enzyme-linked immunosorbent assay for specific diagnosis of canine brucellosis. *J. Clin. Microbiol.* **27**: 837–842.
13. Sieira, R., Comerci, D. J., Sanchez, D. O. and Ugalde, R. A. 2000. A homologue of an operon required for DNA transfer in Agrobacterium is required in *Brucella abortus* for virulence and intracellular multiplication. *J. Bacteriol.* **182**: 4849–4855.

Journal of Reproduction and Development, Vol. 53, No. 6, 2007

—Full Paper—

Transportation of Freeze-Dried Mouse Spermatozoa Under Different Preservation Conditions

Yosuke KAWASE[1)], Takanori TACHIBE[1)], Kou-ichi JISHAGE[1)] and Hiroshi SUZUKI[2,3)]

[1)]Chugai Research Institute for Medical Science, Shizuoka 412-8513, [2)]Research Unit for Functional Genomics, National Research Center for Protozoan Diseases, Obihiro University of Agriculture and Veterinary Medicine, Hokkaido 080-8555 and [3)]Department of Developmental and Medical Technology, Graduate School of Medicine, The University of Tokyo, Tokyo 113-8657, Japan

Abstract. Freeze-dried mouse spermatozoa can be used for normal embryonic development after injection into oocytes, thus indicating that freeze-drying is a useful method for the storage and transportation of genetic materials from animals. We recently reported that storage of freeze-dried mouse spermatozoa requires maintenance at temperatures lower than –80 C for long-term preservation and a pressure of 0.37 mbar at primary drying and that these conditions significantly improve the developmental rate to the blastocyst stage. In this study, we examined the influence of transportation and preservation conditions on freeze-dried spermatozoa. Freeze-dried spermatozoa stored for 2 or 2.5 years at 4 or –80 C were transported round trip overland between Shizuoka and Hokkaido prefectures in Japan or by air between Japan and Belgium. The freeze-drying conditions consisted of primary drying at pressures of 0.04, 0.37 and 1.03 mbar and secondary drying at a pressure of 0.001 mbar. Embryos (2-cell stage) from freeze-dried spermatozoa dried at 0.04 mbar and stored at 4 C for 2 years with and without overland transportation did not develop to term. The development rates of embryos from spermatozoa stored at –80 C for up to 2 years and transported overland, by air and without transportation were 8, 1 and 28%, respectively. The development rates of embryos from spermatozoa without transportation were significantly higher than with transportation ($P<0.05$). These data indicate that freeze-dried spermatozoa stored at –80 C with and without transportation can retain their ability to generate viable offspring after storage for up to 2 years. However, there are limitations to be considered in the transportation of freeze-dried spermatozoa at ambient temperature.

Key words: Freeze-dried spermatozoa, Intra cytoplasmic sperm injection (ICSI), Mouse, Transportation

(**J. Reprod. Dev. 53:** 1169–1174, 2007)

Extensive studies on freeze-dried spermatozoa have been conducted in a variety of species [1]. Especially, research concerning freeze-dried mouse spermatozoa has been reported by many laboratories, and the results indicate that freeze-dried spermatozoa can be used for injection into oocytes with subsequent normal embryonic development after injection [2–8]. Although freeze-dried spermatozoa can be stored and can remain viable after refrigerated (4 C) storage for 1.5 years [6], this length of time is inadequate for maintenance of genetically modified mouse strains and mutant mice in saturation mutagenesis projects. Long-

Accepted for publication: July 10, 2007
Published online: August 13, 2007
Correspondence: H. Suzuki (e-mail: hisuzuki@obihiro.ac.jp)

term (or permanent) preservation of freeze-dried spermatozoa at ambient temperatures would be ideal. However, there are no reports of successful full-term development derived from freeze-dried spermatozoa stored for long-term at room temperature. Recently, we reported that freeze-dried mouse spermatozoa are most efficiently stored for extended periods (extrapolated to several tens of decades) at temperatures lower than −80 C [7]. However, maintaining such low temperatures over a long period of time exposes the samples to risks associated with technical difficulties (e.g., power failure) and requires a relatively high initial investment. Moreover, we have reported that the primary drying pressure is important and influential factor in long-term preservation of freeze-dried mouse spermatozoa at ambient temperatures. A primary drying pressure of 0.37 mbar significantly improves the rate of development to the blastocyst stage [8]. In addition to storage of genetic materials, the conditions for transportation of genetic materials from animals need to be examined. To our knowledge, there is only one report concerning transportation of freeze-dried spermatozoa [2]. The authors reported that a 3-week journey at temperatures varying between 5 and 30 C plus an additional 1-week of storage resulted in 16% of the embryos developing to term after intra cytoplasmic sperm injection (ICSI) with the freeze-dried spermatozoa. The present study was designed to determine the influence of storage temperature, transportation time and primary drying pressure on the development of embryos derived from freeze-dried mouse spermatozoa.

Materials and Methods

Animals

F1 mice (C57BL/6J × C3H/He) were purchased from Clea Japan (Tokyo, Japan). All mice were housed in polycarbonate-cages and maintained under a specific pathogen-free environment in light-controlled (lights on from 0500 to 1900 h) and air-conditioned rooms (temperature, 24 ± 1 C; humidity, 50 ± 10%). The mice had free access to standard laboratory chow (CE-2; Clea Japan). The Institutional Animal Care and Use Committee of Chugai Pharmaceutical reviewed the protocols and confirmed that the animals used in this study were cared for and used under the Guiding Principles for the Care and Use of Research Animals promulgated by them.

Freeze-drying and preservation of spermatozoa

The procedure used for freeze-drying was essentially the same as that described by Kawase *et al.* [7, 8]. Six epididymides from three F1 male mice were removed, and a dense sperm mass was squeezed out of each cauda epididymis from a cut made with scissors. The total sperm mass was gently placed in 9 ml of ethylene glycol bis (beta-aminoethyl ether)-N,N,N',N'-tetraacetic acid (EGTA) Tris-HCl-buffered solution (50 mM EGTA, 50 mM NaCl and 10 mM Tris-HCl, pH 8.0) [4] in a tube (352059; Becton Dickinson Labware, Franklin Lakes, NJ, USA) and kept at 37 C for 10 min. The sperm suspension was divided into 18 aliquots. Each aliquot (500 μl) was placed into an amber vacuum vial for freeze-drying (V-2B; Nichiden-rika Glass, Kobe, Japan). The vials were plunged into liquid nitrogen (approximately −196 C) for 5 min and then transferred to a programmable freeze-dryer (BETA2–16; Martin Christ Gefriertrocknungsanlagen, Osterode am Harz, Germany) that had been precooled to −30 C. The freeze-drying conditions consisted of primary drying at a pressure of 0.04, 0.37 or 1.03 mbar and secondary drying at a pressure of 0.001 mbar. The internal pressure of the vials at the time of sealing was 0.001 mbar; pressure reduction was within 5 min. The vials were stored at 4 or −80 C for about 2 or 2.5 years until transportation and were stored at −80 C until use. Immediately before ICSI, the vials of freeze-dried spermatozoa were unsealed, and the spermatozoa were hydrated by adding 500 μl of sterile distilled water. To maintain a similar composition of the sperm suspension before and after freeze-drying, we added distilled water rather than a medium such as Hepes-buffered culture medium.

Transportation of freeze-dried spermatozoa

Land transportation (Yamato Transport, Tokyo, Japan) consisted of a roundtrip express courier service between Shizuoka and Hokkaido prefectures by train and truck (2,800 km, 5 days, summer season). Air transportation (Japan Airlines, Tokyo, Japan) comprised a roundtrip jet service between Japan and Belgium as check-in baggage (19,000 km, 7 days, winter season).

Monitoring of temperatures during transportation

Temperature was recorded during transporta-

tion at 10-min intervals using a Thermochron data logger (G type; KN Laboratories, Osaka, Japan) and analyzed with the ThermoManager software (KN Laboratories).

Preparation of oocytes

Mature F1 females were induced to superovulate by intraperitoneal injections of 5 IU equine chorionic gonadotrophin (eCG; Serotrophin®, Teikoku Zoki, Tokyo, Japan) followed 48 h later by injection of 5 IU human chorionic gonadotrophin (hCG; Puberogen®, Sankyo, Tokyo, Japan). Freshly ovulated oocytes were collected from their oviducts 15 to 16 h after injection with hCG. The oocytes were treated with 0.1% hyaluronidase (280 U/mg; H-3506; Sigma-Aldrich, St. Louis, MO, USA) in Whitten's medium [9] supplemented with 100 μM ethylene diamine tetraacetic acid disodium salt (EDTA) [10] to remove cumulus cells.

Intracytoplasmic sperm injection

After rehydration of the freeze-dried spermatozoa as described above, one part of the sperm suspension was thoroughly mixed with nine parts 0.9% NaCl solution (saline) containing 12% (w/v) polyvinylpyrrolidone (PVP, No. 99219, Mt. 360,000; Irvine Scientific, Santa Ana, CA, USA). Two drops (approximately 5 μl each) of 12% PVP saline and 2 drops of 20 mM HEPES-buffered Whitten's medium containing 0.1% polyvinyl alcohol (PVA, P-8136, MW 30,000–70,000; Sigma-Aldrich) were linearly placed on the injection chamber [11] and then covered with mineral oil (M-8410, embryo tested; Sigma-Aldrich). The first drop of 12% PVP saline was used to wash the injection pipette, and added to the second drop was 1–2 μl of the diluted sperm suspension. The first drop of the medium was used to remove spermatozoa that had attached to the surface of the injection pipette. The cumulus-free oocytes were placed in the second drop of HEPES-buffered Whitten's medium. The injection chamber with the spermatozoa and oocytes was transferred onto the stage of an inverted microscope maintained at approximately 18 C (MATS-555RSP; Tokai Hit, Shizuoka, Japan).

The procedure for micromanipulation of the sperm for ICSI was essentially the same as described previously [11, 12]. The sperm head was separated from the tail by applying three or four piezo pulses (controller setting: speed 2, intensity 2) to the head-tail junction of the spermatozoon. In a similar manner, 5 isolated sperm heads were lined up in the pipette. Several piezo pulses (controller setting: speed 2, intensity 2) were applied to advance the tip of the injection pipette to the surface of zona pellucida; the pipette was advanced mechanically while applying slight negative pressure. The oolemma was punctured using one piezo pulse (controller setting: speed 1, intensity 1). A single sperm head was then expelled into the ooplasm accompanied by a minimum amount of medium. Following retrieval of as much of the medium as possible, the injection pipette was withdrawn while applying negative pressure to it.

Culture of oocytes and embryos transfer

Sperm-injected oocytes were incubated and cultured in Whitten's medium supplemented with 100 μM EDTA at 37.5 C in a mixture of 5% CO_2 and 95% air. Six hours after ICSI, live oocytes showing two distinct pronuclei and a second polar body were considered fertilized. The fertilized eggs were further cultured under the same conditions. About 24 h after ICSI, the 2-cell embryos were transferred into the oviducts of pseudopregnant ICR recipients (Clea Japan) 0.5 days post coitum (dpc) using the embryo transfer method described by Suzuki *et al.* [13]. The recipient females were sacrificed after 18.5 dpc to determine the number of implantation sites (macroscopic evidence) and the number of term fetuses.

Statistical analysis

The data presented in this study were analyzed statistically by the chi-square test (Table 3) and Tukey's test (Table 2) for nonparametric multiple comparisons (SAS version 6.12; SAS Institute, Cary, NC, USA). In all statistical tests, a difference was considered significant when P was <0.05.

Results

The mean temperature during overland transport was 22 C (range: 17–24 C, Table 1). For air transport between Japan and Belgium, the mean temperature was 18 C with a range of 0.5–27 C (Table 1).

With primary drying of freeze-dried spermatozoa at 0.04 mbar, the embryonic developmental rates to the 2-cell stage from ICSI after storage at 4 C with and without transport were significantly

Table 1. Conditions of transportation of vials of freeze-dried spermatozoa

	Overland	By air
Distance (roundtrip)	2,800 km	19,000 km
Duration	5 days	7 days
Mean temperature	22 C	18 C
Temperature range	17–24 C	0.5–27 C

Temperature was recorded at 10-min intervals using a Thermochron data logger.

Table 2. Fertilization and development of oocytes by ICSI in F1 mice using freeze-dried spermatozoa with a primary pressure of 0.04 mbar

Sperm storage (years)	Storage temperature (C)	Mode of transport	No. of oocytes injected	No. (%) of surviving oocytes	No. (%) of oocytes fertilized[1)]	No. (%) of embryos developed to the 2-cell stage[2)]	No. of 2-cell embryos transferred	No. (%) of implantation sites	No. (%) of live term fetuses
–	–	–	151	109 (72)[a]	106 (97)[a]	103 (97)[a]	103	68 (66)[a]	21 (20)[a]
2	4	–	145	102 (70)[a]	101 (99)[a]	84 (83)[b]	84	3 (4)[b]	0 (0)[b]
2	4	Land	157	101 (64)[a]	98 (97)[a]	81 (83)[b]	81	0 (0)[b]	0 (0)[b]
2	–80	–	155	99 (64)[a]	99 (100)[a]	97 (98)[a]	97	56 (58)[a]	27 (28)[a]
2	–80	Land	150	108 (72)[a]	107 (99)[a]	104 (97)[a]	104	37 (36)[c]	8 (8)[b]
2.5	–80	Air	180	125 (69)[a]	120 (96)[a]	115 (96)[a]	115	7 (6)[b]	1 (1)[b]

[1)]Percentage of surviving oocytes. [2)]Percentage of fertilized oocytes. Values in the same column with different superscripts are significantly different ($P<0.05$).

Table 3. Fertilization and development of oocytes by ICSI using air-transported (Japan↔Belgium) freeze-dried spermatozoa

Vacuum pressure (mbar)	No. of oocytes injected	No. (%) of surviving oocytes	No. (%) of oocytes fertilized[1)]	No. (%) of embryos developed to the 2-cell stage[2)]	No. of 2-cell transferred	No. (%) of implantation sites	No. (%) of live term fetuses
0.04[3)]	180	125 (69)[a]	120 (96)[a]	115 (96)[a]	115	7 (6)[a]	1 (1)[a]
0.37	198	145 (73)[a]	141 (97)[a]	134 (95)[a]	134	43 (32)[b]	22(16)[b]
1.03	180	119 (66)[a]	114 (96)[a]	108 (95)[a]	108	16 (15)[a]	5 (5)[a]

Freeze-dried spermatozoa were stored at –80 C until use. [1)]Percentage of surviving oocytes. [2)]Percentage of fertilized oocytes. [3)]Data from Table 2.

lower than at –80 C ($P<0.05$, Table 2). For storage at –80 C for up to 2 years, the developmental rates to the 2-cell stage were similar for freeze-dried spermatozoa without transport and with either land or air transport ($P>0.05$, Table 2). However, the rate of near full-term fetuses derived from the same conditions (–80 C, storage up to 2 years) but without transportation was 28% and was only 8 and 1% with land and air transport, respectively. No fetuses developed from freeze-dried spermatozoa stored at 4 C (Table 2).

To investigate the effect of air transport and primary drying pressure, we performed ICSI using freeze-dried spermatozoa that had been transported roundtrip between Japan and Belgium after primary drying at pressures of 0.04, 0.37 and 1.03 mbar. The developmental rates to the 2-cell stage were 96, 95 and 95%, respectively. The developmental rates to the 2-cell stage were not significantly different ($P>0.05$, Table 3); however, development to near full-term fetuses at 0.37 mbar was higher than at 0.04 and 1.03 mbar ($P<0.05$, Table 3).

Discussion

The rate of near full-term fetuses using freeze-dried spermatozoa stored at –80 C was significant lower when the samples were transported compared without transport. However, the results showed that freeze-dried spermatozoa stored at –80 C with and without transport can retain their ability to generate viable offspring after storage for up

to 2 years (Table 2). In this study, fertilization and near full-term development were successful using spermatozoa stored for 2.5 years. This storage duration is longer than that reported previously, where live and fertile offspring were obtained from spermatozoa stored for 1.5 years at 4 C [6].

For freeze-dried spermatozoa with primary drying pressure at 0.04 mbar, the embryonic development rates from ICSI to the 2-cell stage with storage at –80 C for 2 and 2.5 years were almost the same as without storage ($P>0.05$, Table 2). The results correspond to the accelerated degradation kinetics determined by the Arrhenius equation [14]; the embryonic development rate from ICSI to the 2-cell stage that would be expected after 100 years of storage at –80 C does not decrease significantly [7]. Consequently, for long-term preservation and transportation after preservation, freeze-dried spermatozoa require storage at –80 C. The embryonic developmental rate (Tables 2 and 3) was influenced mainly by temperature during transportation and to a lesser extent by storage duration. The data show that freeze-dried spermatozoa stored at temperatures lower than –80 C are viable for ICSI; namely, lower temperatures during storage and transportation will result in higher developmental rates.

Primary drying at a pressure of 0.37 mbar had better results than 0.04 or 1.03 mbar after air transport. We previously reported that a pressure of 0.37 mbar significantly improved the rate of development to the blastocyst stage [8]; in the present study, we found that 0.37 mbar significantly improved the rate of development of fetuses to near full-term using freeze-dried spermatozoa with longer term preservation (Table 3). However, the relationship between the primary drying mechanism and embryonic developmental rate was not clarified [8]. Further studies are needed for a better understanding of this relationship.

Further studies are also required to successfully modify the freeze-drying process, including pressure and drying solutions, in order to achieve permanent preservation of mouse spermatozoa at ambient temperature. In addition to the conditions of freeze-drying, the effect of storage time and form of transportation on the development rate of freeze-dried spermatozoa requires further analysis.

Acknowledgments

We thank Ms. S. Uchida, Ms. Y. Nakajima, Mr. H. Tateishi and Mr. T. Hani for technical assistance and Ms. F. Ford for proofreading the manuscript.

References

1. **Suzuki H.** Freeze-dried spermatozoa and freeze-dried sperm injection into oocytes. *J Mamm Ova Res* 2006; 23: 91–95.
2. **Wakayama T, Yanagimachi R.** Development of normal mice from oocytes injected with freeze-dried spermatozoa. *Nature Biotechnol* 1998; 16: 639–641.
3. **Kusakabe H, Szczygiel MA, Whittingham DG, Yanagimachi R.** Maintenance of genetic integrity in frozen and freeze-dried mouse spermatozoa. *Proc Natl Acad Sci USA* 2001; 98: 13501–13506.
4. **Kaneko T, Whittingham DG, Yanagimachi R.** Effect of pH value of freeze-drying solution on the chromosome integrity and developmental ability of mouse spermatozoa. *Biol Reprod* 2003; 68: 136–139.
5. **Kaneko T, Whittingham DG, Overstreet JW, Yanagimachi R.** Tolerance of the mouse sperm nuclei to freeze-drying depends on their disulfide status. *Biol Reprod* 2003; 69: 1859–1862.
6. **Ward MA, Kaneko T, Kusakabe H, Biggers JD, Whittingham DG, Yanagimachi R.** Long-term preservation of mouse spermatozoa after freeze-drying and freezing without cryoprotection. *Biol Reprod* 2003; 69: 2100–2108.
7. **Kawase Y, Araya H, Kamada N, Jishage K, Suzuki H.** Possibility of long-term preservation of freeze-dried mouse spermatozoa. *Biol Reprod* 2005; 72: 568–573.
8. **Kawase Y, Hani T, Kamada N, Jishage K, Suzuki H.** Effect of pressure at primary drying of freeze-drying mouse sperm reproduction ability and preservation potential. *Reproduction* 2007; 133: 841–846.
9. **Whitten WK.** Nutrient requirements for the culture of preimplantation embryos *in vitro*. *Adv Biosci* 1971; 6: 129–141.
10. **Abramczuk J, Solter D, Koprowski H.** The beneficial effect of EDTA on development of mouse one-cell embryos in chemically defined medium. *Develop Biol* 1977; 61: 378–383.
11. **Kawase Y, Iwata T, Toyoda Y, Wakayama T, Yanagimachi R, Suzuki H.** Comparison of intracytoplasmic sperm injection of inbred and hybrid mice. *Mol Reprod Develop* 2001; 60: 74–78.

12. **Kimura Y, Yanagimachi R.** Intracytoplasmic sperm injection in the mouse. *Biol Reprod* 1995; 52: 709–720.
13. **Suzuki H, Ueda O, Kamada N, Jishage K, Katho M, Shino M.** Improved embryo transfer into the oviduct by local application of a vasoconstrictor in mice. *J Mamm Ova Res* 1994; 11: 19–53.
14. **Some IT, Bogaerts P, Hanocq M, Dubois J.** Incorporating batch effects in the estimation of drug stability parameters using an Arrhenius model. *Intl J Pharmacol* 1999; 184: 165–172.

BIOLOGY OF REPRODUCTION 77, 954–959 (2007)
Published online before print 5 September 2007.
DOI 10.1095/biolreprod.107.060293

Embryo Spacing and Implantation Timing Are Differentially Regulated by LPA3-Mediated Lysophosphatidic Acid Signaling in Mice[1]

Kotaro Hama,[4] Junken Aoki,[2,3,4,6] Asuka Inoue,[4] Tomoko Endo,[4] Tomokazu Amano,[5] Rie Motoki,[4] Motomu Kanai,[4] Xiaoqin Ye,[8] Jerold Chun,[7] Norio Matsuki,[4] Hiroshi Suzuki,[5,9] Masakatsu Shibasaki,[4] and Hiroyuki Arai[4]

Graduate School of Pharmaceutical Sciences[4] and Department of Developmental and Medical Technology,[5] Graduate School of Medicine, The University of Tokyo, Tokyo 113-0033, Japan
PRESTO,[6] Japan Science and Technology Corporation, Saitama 32-0012, Japan
Helen L. Dorris Institute for Childhood and Adolescent Neuropsychiatric Disorders,[7] The Scripps Research Institute,[8] La Jolla, California 92037
Obihiro University of Agriculture and Veterinary Medicine,[9] Obihiro, Hokkaido 080-8555, Japan

ABSTRACT

In polytocous animals, blastocysts are evenly distributed along each uterine horn and implant. The molecular mechanisms underlying these precise events remain elusive. We recently showed that lysophosphatidic acid (LPA) has critical roles in the establishment of early pregnancy by affecting embryo spacing and subsequent implantation through its receptor, LPA3. Targeted deletion of *Lpa3* in mice resulted in delayed implantation and embryo crowding, which is associated with a dramatic decrease in the prostaglandins and prostaglandin-endoperoxide synthase 2 expression levels. Exogenous administration of prostaglandins rescued the delayed implantation but did not rescue the defects in embryo spacing, suggesting the role of prostaglandins in implantation downstream of LPA3 signaling. In the present study, to know how LPA3 signaling regulates the embryo spacing, we determined the time course distribution of blastocysts during the preimplantation period. In wild-type (WT) uteri, blastocysts were distributed evenly along the uterine horns at Embryonic Day 3.8 (E3.8), whereas in the *Lpa3*-deficient uteri, they were clustered in the vicinity of the cervix, suggesting that the mislocalization and resulting crowding of the embryos are the cause of the delayed implantation. However, embryos transferred singly into E2.5 pseudopregnant *Lpa3*-deficient uterine horns still showed delayed implantation but on-time implantation in WT uteri, indicating that embryo spacing and implantation timing are two segregated events. We also found that an LPA3-specific agonist induced rapid uterine contraction in WT mice but not in *Lpa3*-deficient mice. Because the uterine contraction is critical for embryo spacing, our results suggest that LPA3 signaling controls embryo spacing via uterine contraction around E3.5.

embryo spacing, female reproductive tract, growth factors, implantation, LPA3, lysophosphatidic acid, signal transduction, uterus

INTRODUCTION

Implantation is a series of processes that are regulated by various kinds of signaling pathways between the embryo and the uterus during the initial period of gestation. Implantation consists of positioning, attachment, and invasion of the embryo (blastocyst) in the uterus [1–3]. In many polytocous species (species that have many offspring in a single birth), the embryos are distributed evenly rather than randomly along the uterus. Preformed implantation sites could have been a possible explanation for the even distribution of blastocysts, although this hypothesis is inconsistent with the finding that the implantation sites are equidistant along the uterine horn, irrespective of the number of blastocysts transferred into the uterus [4]. In rabbits, blastocysts were found to enter the uterus at Embryonic Day 3 (E3.0), move rapidly from E3.0 to E5.0, move slowly and align equidistantly around E6.0, and finally implant around E7.0 [4]. Thus, it is likely that there are at least two events for the completion of implantation. First, blastocysts align equidistantly along the uterus (spacing), and then they implant (implantation).

Several previous reports gave some insight into the molecular mechanisms regulating the spacing and the implantation. Administration of relaxin (a potent inhibitor of myometrial activity) in rats was found to disrupt the normal distribution of the blastocysts before implantation [5, 6]. In addition, the frequency of myometrial contractions in pregnant rats was significantly higher in the immediate preimplantation period than in the rest of the postimplantation period [7]. These observations indicated that myometrial activity in the uterus is at least partly responsible for proper embryo spacing. Several bioactive molecules have been found to regulate the implantation through their corresponding cellular receptors. These include ovarian steroid hormones, prostaglandins (PGs), and lysophosphatidic acid (LPA). Administration of a progesterone receptor antagonist to pregnant mice prevented implantation without affecting the development of blastocysts [8]. In addition, implantation was found to be defective in mice and rats treated with indomethacin, an inhibitor of PG-endoperoxide synthase (PTGS), a critical enzyme for PG biosynthesis, as well as in PTGS2-deficient mice [9–11]. Consistent with these

[1]Supported by grants to J.A. and H.A. from the National Institute of Biomedical Innovation, PRESTO (Japan Science and Technology Corporation), the 21st Century Center of Excellence Program, and the Ministry of Education, Science, Sports, and Culture of Japan, and to J.C. from the National Institutes of Health, Bethesda, Maryland (NIH ROI HD050685).
[2]Correspondence: FAX: 81 22 795 6859;
e-mail: jaoki@mail.pharm.tohoku.ac.jp
[3]Current address: Graduate School of Pharmaceutical Sciences, Tohoku University, 6-3, Aoba, Aramaki, Aoba-ku, Sendai, Miyagi 980-8578, Japan.

Received: 23 January 2007.
First decision: 23 February 2007.
Accepted: 9 August 2007.

ISSN: 0006-3363. http://www.biolreprod.org

PTGS studies, implantation was found to fail in cytosolic phospholipase A_2alpha (PLA2G4A) knockout mice [12]. PLA2G4A is a major provider of arachidonic acid for the PTGS system in PG synthesis. These results suggest a pivotal role of ovarian steroid hormones and PGs in implantation.

Among the above-mentioned bioactive molecules that are possibly involved in early implantation events, LPA (1- or 2-acyl-LPA) may also be important, because it influences both the spacing and the implantation. LPA is a simple phospholipid that mediates multiple cellular processes both in vivo and in vitro through at least five G protein-coupled receptors specific to LPA (LPA1/EDG2/vzg-1, LPA2/EDG4, LPA3/EDG7, LPA4/GPR23, and LPA5/GPR92) [13–17]. The in vitro actions include platelet aggregation, cell migration, cell proliferation, and cytoskeletal reorganization [18]. LPA also stimulates ovum transport and maturation of oocytes, suggesting that it has roles in female reproductive organs [19, 20]. Experiments with LPA receptor knockout mice showed that LPA signaling has very important roles in both physiological and pathological conditions, such as neural development (LPA1), neuropathic pain (LPA1), diarrhea (LPA2), and implantation (LPA3) [21–24].

In *Lpa3*-deficient uteri, implantation sites, which are normally detectable at E4.5, were completely absent at E4.5 but detectable at E5.5 (delayed implantation). In addition, the implantation sites in $Lpa3^{-/-}$ uteri were unevenly distributed [24]. As a result, $Lpa3^{-/-}$ female mice showed significantly reduced litter sizes, which could be attributed to the delayed implantation and the altered embryo spacing [24]. Interestingly, around E3.5, *Lpa3* expression is up-regulated transiently by the action of an ovarian hormone, progesterone, which has critical roles in the establishment of early pregnancy, including implantation [25]. In addition, the expression of PTGS-2, as well as of PG levels, was up-regulated around E3.5, which was not observed in *Lpa3*-deficient uteri. Administration of PGs (prostaglandin E_2 [PGE_2] and carbaprostacyclin [cPGI], a stable analog of prostacyclin) into E3.5 *Lpa3*-deficient females could restore the delayed implantation [24]. Thus, it is likely that PGs are the effectors of the progesterone-regulated LPA3 signaling. However, PGE_2 and cPGI administration did not correct the embryo crowding in *Lpa3*-deficient females [24], indicating that embryo spacing is regulated differentially from embryo implantation downstream of LPA3-mediated signaling. In the present study, to obtain insights into the mechanism underlying embryo spacing, we examined the role of LPA3 signaling in embryo spacing and uterine contraction in the preimplantation period.

MATERIALS AND METHODS

Mice

The *Lpa3* gene was originally disrupted by homologous recombination, as described previously [24]. Heterozygous mice were intercrossed, and the resulting $Lpa3^{+/+}$ or $Lpa3^{-/-}$ mice were used for analysis. All mice used in the present study were of mixed background (129/SvJ and C57BL/6J). Mice were bred and maintained at the Animal Care Facility in the Graduate School of Pharmaceutical Sciences, the University of Tokyo, under specific pathogen-free conditions in accordance with institutional guidelines.

Measurements of Embryo Distribution

Wild-type (WT) or *Lpa3*-deficient mice were mated with fertile WT males (E0.5 = vaginal plug, 1200 h). On E3.5 (1200 h), E3.8 (1900 h), or E4.5 (1200 h), mice were i.v. perfused with 4% paraformaldehyde for fixation. Then, the whole uterus was carefully excised and embedded in paraffin wax. Longitudinal sequential sections were stained with hematoxylin and eosin to identify the blastocysts. The distance between each blastocyst was calculated by National Institutes of Health image software.

Blastocysts and Transfer into Uterus

Females were mated with vasectomized males to induce pseudopregnancy. On E2.5, the eight-cell embryos were collected from pregnant WT mice and cultured in KSOM medium (Millipore, Billerica, MA) overnight and then transferred to the uteri of pseudopregnant recipients on E2.5. Implantation sites on E4.5 were localized by i.v. injection of Evans blue dye (200 μl, 1% in 1× PBS; Sigma, St. Louis, MO) [26]. For PG treatment, *Lpa3*-deficient female mice were i.p. administrated with vehicle (10% EtOH with saline) or PGs (5 μg of PGE_2 and 5 μg of cPGI) at 1000 and 1800 h on E3.5.

Measurements of Uterine Contraction

The uteri from WT or *Lpa3*-deficient mice on E3.5 were removed carefully to avoid excessive stretching; each was placed in a Petri dish containing Krebs solution (118 mM NaCl, 4.5 mM KCl, 1.0 mM $MgSO_2$, 1.0 mM KH_2PO_4, 25 mM $NaHCO_3$, 1.8 mM $CaCl_2$, and 6.0 mM glucose), and excessive tissue was removed. The mechanical activity of the uterine samples was recorded continuously under isometric conditions. Each sample was connected to a force displacement transducer (model TB-612T; Nihon Kohden Co., Ltd., Tokyo, Japan) coupled to a multichannel amplifier (model MEG-6108; Nihon Kohden), and mounted in a 10-ml organ bath with Krebs solution suffused with 95% O_2:5% CO_2 at 37°C. Each sample was allowed to equilibrate for 30 min under an initial load of 1.0 g. The myometrial contractility was recorded before and after the addition of 10 μM T13, an LPA3-selective agonist [27], and later 10 μM acetylcholine.

Statistical Analysis

Results are expressed as means ± SD. The data were analyzed with the Student *t*-test. $P < 0.05$ was considered significant.

RESULTS

Aberrant Embryo Spacing During Peri-Implantation Period in Lpa3-Deficient Mice

In mice, embryos in the late morula stage or early blastocyst stage enter the uterus around E3.0. The blastocysts begin to interact with the uterine luminal epithelium around E3.5 and implant around E4.0. To pinpoint the time when the blastocysts are distributed along the uterine horn, we determined the locations of blastocysts along the uterine horns during E3.0–E3.8. The axial transverse and sequential hematoxylin and eosin-stained uterine sections from both WT and $Lpa3^{-/-}$ mice during E3.0–E3.8 were examined (Fig. 1a). The presence and locations of blastocysts along the uterine horns were determined under microscopy (Fig. 1a). The location is expressed as the percentage of the uterine length from the uterotubal junction (Fig. 1b), and the degree of equidistance is shown as a coefficient of variation, which is the mean of the distances between blastocysts in a horn divided into the standard deviation (Fig. 1c). On E3.0, most blastocysts were located in the vicinity of the uterotubal junction both in WT and $Lpa3^{-/-}$ uteri (data not shown). On E3.5, most of the blastocysts were distributed evenly in most of the WT uteri, although some of them were still present in clusters (Fig. 1, a–c). By contrast, most blastocysts in $Lpa3^{-/-}$ uteri clustered in the vicinity of the uterotubal junction, although some were found near the cervix (Fig. 1, a–c). On E3.8, blastocysts were evenly distributed in almost all uteri in WT mice, whereas they were not evenly distributed in $Lpa3^{-/-}$ uteri (Fig. 1, a–c). The cluster of blastocysts was similar to the implantation sites seen at E5.5 in $Lpa3^{-/-}$ uteri [24]. These data demonstrate that LPA3-mediated signaling is required at least for embryo spacing during the preimplantation period and that embryo spacing occurs before embryo implantation.

LPA3-Mediated Signaling on Uterine Contraction

Myometrial activity is important for both the transport and spacing of the preimplantation embryos [4–6]. Thus, we

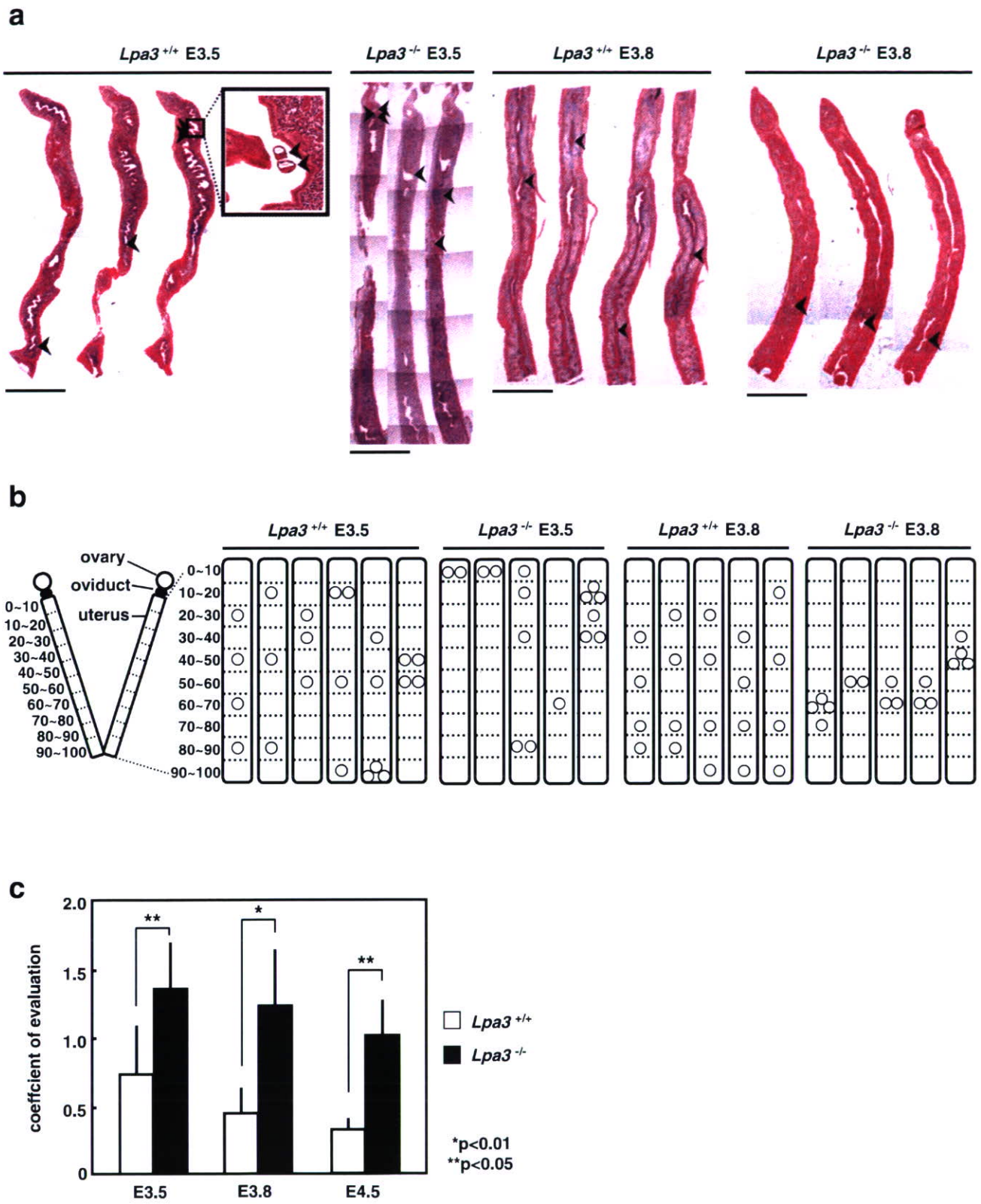

FIG. 1. Distribution of embryos in *Lpa3*-deficient uteri is uneven. **a**) Sequential histopathological pictures of longitudinal section with blastocysts for each time point. Arrowheads point to the blastocyst location. Representative experiment was shown for each time. Bar = 5 mm. **b**) Schematic localization of embryos along WT (wild-type, labeled *Lpa3*$^{+/+}$) and *Lpa3*-deficient (*Lpa3*$^{-/-}$) uterine horns at E3.5 and E3.8. Data were obtained from the axial transverse and sequential hematoxylin and eosin-stained sections. The location of blastocysts is represented by the percentage of uterine length from the uterotubal junction. **c**) The degree of equidistance is expressed as a coefficient of evaluation, which is the mean of the distances between blastocysts in a horn divided into the standard deviation.

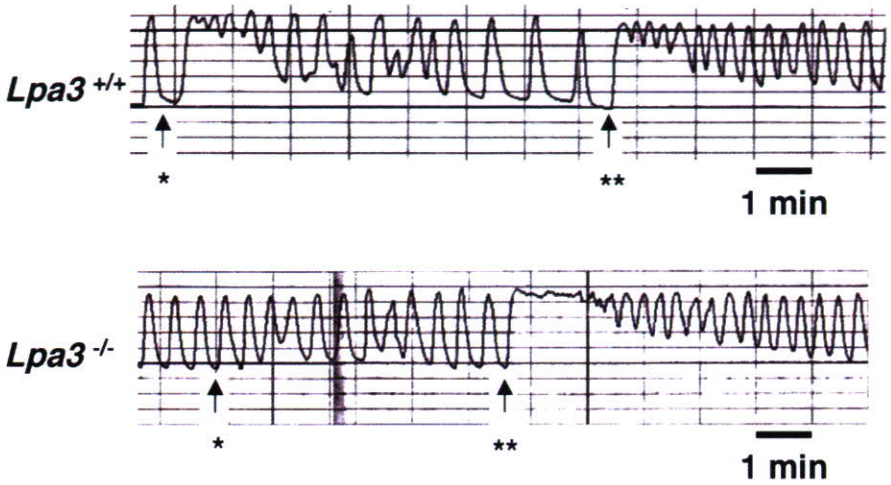

FIG. 2. LPA3-specific agonist, T13, induced uterine contraction through LPA3. Uterine contractile activity upon 10 μM T13 (*) or 10 μM acetylcholine (**) treatment in isolated E3.5 WT or *Lpa3*$^{-/-}$ uteri. Resting applied tension was 1.0 g. At least four independent experiments were performed, and a representative experiment is shown.

examined the effects of LPA3-mediated signaling on myometrial activity with T13 [27]. T13 induced a potent contractile response on isolated E3.5 WT uteri (Fig. 2). However, this contractile response was completely absent in isolated E3.5 *Lpa3*-deficient uteri (Fig. 2). The E3.5 *Lpa3*-deficient uteri contracted normally in response to acetylcholine, a potent inducer of uterine contraction (Fig. 2), indicating that the *Lpa3*-deficient uteri lose LPA3 agonist-induced contraction but retain uterine myometrial contractility per se. These data raise the possibility that LPA3 signaling regulates embryo spacing through uterine contraction during the preimplantation period.

Effect of Embryonic Crowding on Implantation Timing

We show that embryo spacing occurs prior to embryo implantation (Fig. 1b). *Lpa3*-deficient females have defects in both embryo spacing and implantation timing [24]. These results raise the possibility that embryo crowding is responsible for the delayed implantation in the *Lpa3*-deficient uterus. We previously showed that multiple embryos (three to four in each uterine horn) transferred into pseudopregnant *Lpa3*$^{-/-}$ uteri resulted in delayed implantation and uneven distribution of implantation sites at E5.5 [24]. To eliminate any potential influence of embryo crowding on implantation, we transferred a single WT embryo into each E2.5 WT or *Lpa3*-deficient pseudopregnant uterine horn. One implantation site could be consistently detected in 9 of 10 transferred uterine horns in WT mice. By contrast, no implantation site was ever observed in *Lpa3*$^{-/-}$ mice (Fig. 3), whereas the transferred embryo, which was collected by flushing each uterine horn on E4.5, was found to be well developed and had already hatched (data not shown). These results clearly demonstrate that the singly-transferred embryos still had delayed implantation in the *Lpa3*-deficient uteri but on-time implantation in WT uteri (Fig. 3), indicating that delayed implantation in *Lpa3*-deficient uteri is an event independent of embryo crowding. Furthermore, this aberrant implantation timing was rescued by the exogenous administration of PGE_2 and cPGI into E3.5 *Lpa3*-deficient females (data not shown). These data show that embryo spacing and implantation timing are two segregated events, meaning that LPA3-mediated signaling controls embryo spacing around E3.5 and independently regulates the implantation timing thereafter.

DISCUSSION

Our recent study demonstrated a critical role of LPA3-mediated LPA signaling in embryo implantation. Targeted deletion of *Lpa3* was shown to cause delayed implantation, altered embryo spacing, significantly reduced litter size in female mice, and activation of the PG synthetic pathway, and the resulting PGs were shown to be involved in the implantation process downstream of LPA3 signaling [24]. However, it is unclear whether LPA3-mediated LPA signaling regulates implantation timing and embryo spacing independently or whether it controls one event that subsequently influences the other. In the present study, we have further demonstrated that LPA3-mediated LPA signaling regulates implantation timing and embryo spacing independently (Fig. 4).

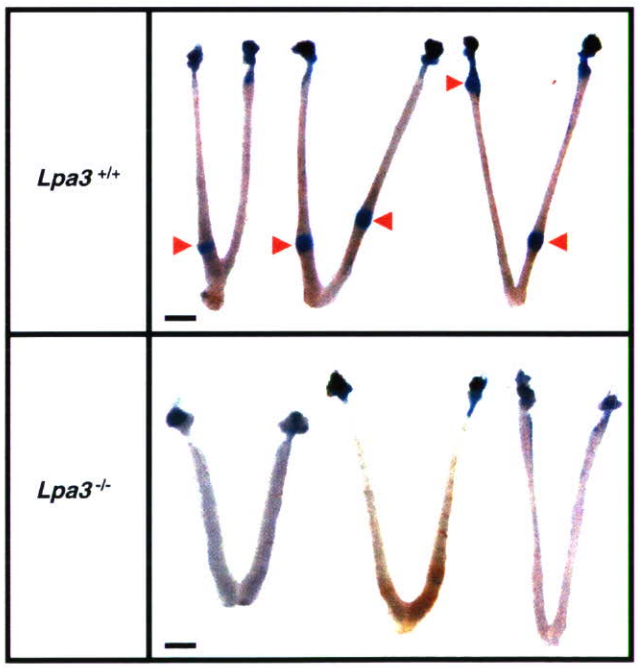

FIG. 3. Embryo crowding is not the cause for delayed implantation in *Lpa3*$^{-/-}$ uteri. A single blastocyst was injected into a pseudopregnant uterine horn in both WT and *Lpa3*$^{-/-}$ mice at E2.5. Detection of singly-transferred embryos in WT and *Lpa3*-deficient uteri at E4.5 was performed by blue dye injection. Red arrowheads show the implantation sites. Ten experiments were performed for both WT and *Lpa3*$^{-/-}$ mice, and representative experiments are shown. Bar = 5 mm.

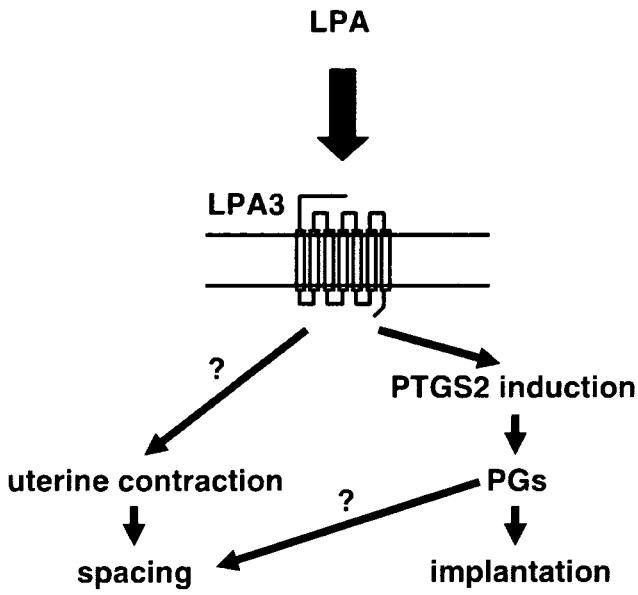

FIG. 4. LPA3-mediated signaling regulates both embryo spacing and implantation independently. Proposed model of LPA3-mediated signaling in embryo spacing and implantation. LPA3-mediated signaling can stimulate uterine contraction and regulate embryo spacing around E3.5 through unknown mechanisms. It also determines implantation timing thereafter via PTGS2-derived prostaglandins (PGs).

Previous studies have demonstrated that myometrial contraction is critical for proper embryonic spacing. In the present study, we showed that LPA induced uterine myometrial contraction via LPA3 because an LPA3-specific agonist, T13, induced uterine myometrial contraction in WT uteri but not in *Lpa3*-deficient uteri. Thus, it might be speculated that LPA3-mediated signaling regulates embryo spacing through its effect on uterine contraction. We recently showed that *Lpa3* expression in uteri dramatically changes during the estrus cycle and is up-regulated at E2.5–3.5 [24, 25]. In addition, the *Lpa3* expression in uteri is dependent on progesterone, an ovarian hormone that has a critical role in the establishment of early pregnancy, including implantation. Recent findings indicate that uterus activity is controlled by steroid hormones, including progesterone [28]. Thus, progesterone may regulate *Lpa3* expression, thereby contributing to uterus function during early pregnancy. At present, the molecular mechanism by which LPA3 activation leads to uterine contraction remains unknown (Fig. 4). PG, which induces the contraction of smooth muscle, can be a favoring factor in LPA3-mediated uterine contraction (Fig. 4), because it has already been shown to be essential in embryo spacing [9–12]. Further studies are necessary to identify the linkage of LPA3 and PG signaling in embryo implantation.

A problem with treatments for infertility by assisted reproductive technologies (ART) is that the implantation rate is poor [29]. Moreover, certain abnormal pregnancies, such as ectopic pregnancy and placenta previa, are associated with the mislocation of zygotes in the uterus. It is possible that these abnormal pregnancies are due to attenuated LPA3 signaling. LPA3 is a potential therapeutic target that promotes implantation in ART and that prevents such abnormal pregnancies.

In conclusion, we showed that LPA3 signaling regulates the uterine contraction, which can control the embryo spacing. Thus, in the establishment of early pregnancy, LPA3 signaling regulates two events: the embryo implantation mediated by PG signaling and the embryo spacing induced by uterine contraction.

REFERENCES

1. Wang H, Dey SK. Lipid signaling in embryo implantation. Prostaglandins Other Lipid Mediat 2005; 77:84–102.
2. Dey SK, Lim H, Das SK, Reese J, Paria BC, Daikoku T, Wang H. Molecular cues to implantation. Endocr Rev 2004; 25:341–373.
3. Carson DD, Bagchi I, Dey SK, Enders AC, Fazleabas AT, Lessey BA, Yoshinaga K. Embryo implantation. Dev Biol 2000; 223:217–237.
4. Boving BG. Biomechanics of implantation. In: Blandau RJ (ed.), The Biology of the Blastocyst. Chicago: The University of Chicago Press; 1971:423–442.
5. Pusey J, Kelly WA, Bradshaw JM, Porter DG. Myometrial activity and the distribution of blastocysts in the uterus of the rat: interference by relaxin. Biol Reprod 1980; 23:394–397.
6. Rogers PA, Murphy CR, Squires KR, MacLennan AH. Effects of relaxin on the intrauterine distribution and antimesometrial positioning and orientation of rat blastocysts before implantation. J Reprod Fertil 1983; 68: 431–435.
7. Crane LH, Martin L. In vivo myometrial activity during early pregnancy and pseudopregnancy in the rat. Reprod Fertil Dev 1991; 3:233–244.
8. Roblero LS, Fernandez O, Croxatto HB. The effect of RU486 on transport, development and implantation of mouse embryos. Contraception 1987; 36:549–555.
9. Kennedy TG. Evidence for a role for prostaglandins in the initiation of blastocyst implantation in the rat. Biol Reprod 1977; 16:286–291.
10. Kinoshita K, Satoh K, Ishihara O, Tsutsumi O, Nakayama M, Kashimura F, Mizuno M. Involvement of prostaglandins in implantation in the pregnant mouse. Adv Prostaglandin Thromboxane Leukot Res 1985; 15: 605–607.
11. Lim H, Paria BC, Das SK, Dinchuk JE, Langenbach R, Trzaskos JM, Dey SK. Multiple female reproductive failures in cyclooxygenase 2-deficient mice. Cell 1997; 91:197–208.
12. Song H, Lim H, Paria BC, Matsumoto H, Swift LL, Morrow J, Bonventre JV, Dey SK. Cytosolic phospholipase A2alpha is crucial [correction of A2alpha deficiency is crucial] for 'on-time' embryo implantation that directs subsequent development. Development 2002; 129:2879–2889.
13. An S, Bleu T, Zheng Y, Goetzl EJ. Recombinant human G protein-coupled lysophosphatidic acid receptors mediate intracellular calcium mobilization. Mol Pharmacol 1998; 54:881–888.
14. Bandoh K, Aoki J, Hosono H, Kobayashi S, Kobayashi T, Murakami MK, Tsujimoto M, Arai H, Inoue K. Molecular cloning and characterization of a novel human G-protein-coupled receptor, EDG7, for lysophosphatidic acid. J Biol Chem 1999; 274:27776–27785.
15. Hecht JH, Weiner JA, Post SR, Chun J. Ventricular zone gene-1 (vzg-1) encodes a lysophosphatidic acid receptor expressed in neurogenic regions of the developing cerebral cortex. J Cell Biol 1996; 135:1071–1083.
16. Noguchi K, Ishii S, Shimizu T. Identification of p2y9/GPR23 as a novel G protein-coupled receptor for lysophosphatidic acid, structurally distant from the Edg family. J Biol Chem 2003; 278:25600–25606.
17. Lee CW, Rivera R, Gardell S, Dubin AE, Chun J. GPR92 as a new G12/13- and Gq-coupled lysophosphatidic acid receptor that increases cAMP, LPA5. J Biol Chem 2006; 281:23589–23597.
18. Contos JJ, Ishii I, Chun J. Lysophosphatidic acid receptors. Mol Pharmacol 2000; 58:1188–1196.
19. Hinokio K, Yamano S, Nakagawa K, Iraharaa M, Kamada M, Tokumura A, Aono T. Lysophosphatidic acid stimulates nuclear and cytoplasmic maturation of golden hamster immature oocytes in vitro via cumulus cells. Life Sci 2002; 70:759–767.
20. Kunikata K, Yamano S, Tokumura A, Aono T. Effect of lysophosphatidic acid on the ovum transport in mouse oviducts. Life Sci 1999; 65:833–840.
21. Contos JJ, Fukushima N, Weiner JA, Kaushal D, Chun J. Requirement for the lpA1 lysophosphatidic acid receptor gene in normal suckling behavior. Proc Natl Acad Sci U S A 2000; 97:13384–13389.
22. Inoue M, Rashid MH, Fujita R, Contos JJ, Chun J, Ueda H. Initiation of neuropathic pain requires lysophosphatidic acid receptor signaling. Nat Med 2004; 10:712–718.
23. Li C, Dandridge KS, Di A, Marrs KL, Harris EL, Roy K, Jackson JS, Makarova NV, Fujiwara Y, Farrar PL, Nelson DJ, Tigyi GJ, et al. Lysophosphatidic acid inhibits cholera toxin-induced secretory diarrhea through CFTR-dependent protein interactions. J Exp Med 2005; 202:975–986.
24. Ye X, Hama K, Contos JJ, Anliker B, Inoue A, Skinner MK, Suzuki H,

Amano T, Kennedy G, Arai H, Aoki J, Chun J. LPA3-mediated lysophosphatidic acid signalling in embryo implantation and spacing. Nature 2005; 435:104–108.
25. Hama K, Aoki J, Bandoh K, Inoue A, Endo T, Amano T, Suzuki H, Arai H. Lysophosphatidic receptor, LPA3, is positively and negatively regulated by progesterone and estrogen in the mouse uterus. Life Sci 2006; 79:1736–1740.
26. Paria BC, Huet HY, Dey SK. Blastocyst's state of activity determines the "window" of implantation in the receptive mouse uterus. Proc Natl Acad Sci U S A 1993; 90:10159–10162.
27. Tamaruya Y, Suzuki M, Kamura G, Kanai M, Hama K, Shimizu K, Aoki J, Arai H, Shibasaki M. Identifying specific conformations by using a carbohydrate scaffold: discovery of subtype-selective LPA-receptor agonists and an antagonist. Angew Chem Int Ed Engl 2004; 43:2834–2837.
28. Mueller A, Maltaris T, Siemer J, Binder H, Hoffmann I, Beckmann MW, Dittrich R. Uterine contractility in response to different prostaglandins: results from extracorporeally perfused non-pregnant swine uteri. Hum Reprod 2006; 21:2000–2005.
29. Christiansen OB, Nielsen HS, Kolte AM. Future directions of failed implantation and recurrent miscarriage research. Reprod Biomed Online 2006; 13:71–83.

Vitrification of Canine Oocytes

Yasuyuki Abe[1], Dong-Soo Lee[1], Sang-Keun Kim[2] and Hiroshi Suzuki[1, 3*]

[1]Obihiro University of Agriculture and Veterinary Medicine, Inada-cho, Obihiro, Hokkaido 080-8555, Japan

[2]College of Veterinary Medicine, Chungnam National University, Yuseong-gu, Daejeon 305-764, Korea

[3]Department of Developmental and Medical Technology, Graduate School of Medicine, The University of Tokyo, Tokyo 113-0033, Japan

*To whom correspondence should be addressed. e-mail: hisuzuki@obihiro.ac.jp

Abstract: The objective of the present study was to compare the vitrification method for cryopreservation of canine oocytes. Canine cumulus-oocyte complexes (COCs) were collected from ovaries, and were vitrified by ethylene glycol based (E30S) or DMSO based (DAP213) methods. In the E30S method, COCs were exposed to the vitrification solution, composed of 30% ethylene glycol and 0.5 M sucrose, step-wise transferred onto a cryotop holder, then plunged directly into liquid nitrogen. In the DAP213 method, COCs were exposed to 1 M DMSO and DAP213 solution in a cryotube, and thereafter plunged directly into liquid nitrogen. Although vitrified-warmed COCs in the E30S method showed fewer morphological abnormalities, and higher viability than those in the DAP213 method, there was no significant difference in between. These results indicate that either method of vitrification is available and statistically comparable for cryopreservation of canine oocytes.

Key words: Dog, Oocyte, Vitrification, Cryopreservation

Introduction

Assisted reproductive techniques (ART) of canine species such as in vitro maturation (IVM), culture and cryopreservation of the genetic resource materials have limited application *per se*, when compared to those for other experimental and domestic animals. However, they can be useful for improved breeding of companion and working dogs, including guide dogs for the blind. Although guide dogs remarkably contribute to the improvement of the quality of life of blind people in the world, many countries suffer from an acute shortage of guide dogs. Even among Labrador Retrievers, which are particularly suited to the role, only 30-40% of the dogs that are trained become guide dogs in Japan. Current figures indicate that approximately 950 dogs are actively engaged in guiding blind people, however, this number is low in light of the estimated demand, which ranges between 4,800-7,800, including latent needs in Japan. ART would help make it possible to overcome one of the problems. Although there are some reports on IVM of oocytes and culture of embryos in [1, 2], no attempt has been made to cryopreserve canine oocytes and embryos, and then perform embryo transfer (ET). Vitrification has been widely developed to apply to cryopreservation of mammalian embryos. In the mouse, embryo cryopreservation by a vitrification method utilizing a sampling tube with DAP213 solution (2 M dimethyl sulfoxide, 1 M acetamide, and 3 M propylene glycol) as a vitrification solution (DAP213 method) has been proven successful [3]. Moreover, it is possible to vitrify canine ovarian tissues by the DAP213 method [4]. Porcine oocytes were vitrified successfully using a cryotop sheet following exposure to vitrification solution by the step-wise method (E30S method) [5]. However, the suitability of both vitrification methods for canine embryos has not been investigated.

The objective of the present study was to compare the DAP213 with E30S methods for vitrification of canine germinal vesicle (GV) stage oocytes, to improve the breeding management programs for guide dogs for the blind.

Materials and Methods

Collection of cumulus oocyte complexes (COCs)

Ovaries within the ovarian bursa from bitches of mixed breed at random stages of the estrous cycle were collected at slaughterhouses and transported to the laboratory in a thermos flask containing sterile saline at approximately 37°C. Each ovary was cleaned of fat and blood vessels and placed in a Petri dish containing TCM199 medium (Gibco-Invitrogen Life Technologies, NY, USA) supplemented with 10% fetal calf serum, 100 units/ml penicillin G potassium (Meiji, Tokyo, Japan) and 100 μg/ml streptomycin sulfate (Meiji, Tokyo, Japan), for further dissection. Ovarian tissue was sliced by a surgical blade (Feather, Osaka, Japan) repeatedly to collect COCs. Only COCs with more than two layers of cumulus cells and a homogeneous dark cytoplasm ≥100 μm in diameter were used in this study. All chemicals were purchased from Sigma Chemical Co. (St. Louis, MO USA) except for those specifically described.

The tissues and cells derived from animals used in this study were treated under the Guiding Principles for the Care and Use of Research Animals established by Obihiro University of Agriculture and Veterinary Medicine.

Vitrification and Thawing

DAP213 method

The COCs were pretreated with PB1 medium [6] containing 1 M dimethyl sulfoxide (DMSO) at room temperature (23±2 °C). The COCs were transferred into a 1 ml cryotube (Nalge Nunc International, Tokyo, Japan) containing 5 μl of 1 M DMSO, which was then placed in ice water for 5 min to allow DMSO to thoroughly bathe the COCs.